Heat and charge transport in YNi_2B_2C and $HoNi_2B_2C$ single crystals

2008 J. Phys.: Condens. Matter 20 175221

(http://iopscience.iop.org/0953-8984/20/17/175221)

J. Phys.: Condens. Matter **20** (2008) 175221 (7pp) doi:10.1088/0953-8984/20/17/175221

Heat and charge transport in YNi_2B_2C and $HoNi_2B_2C$ single crystals

M Schneider[1,2], A Gladun[1,3], A Kreyssig[1,5], J Wosnitza[4], V Petzold[3,6], H Rosner[3], G Behr[2], D Souptel[2], K-H Müller[2], S-L Drechsler[2] and G Fuchs[2]

[1] Institut für Festkörperphysik, Technische Universität Dresden, D-01062 Dresden, Germany
[2] Leibniz-Institut für Festkörper- und Werkstoffforschung Dresden (IFW), D-01171 Dresden, Germany
[3] Max-Planck-Institut für Chemische Physik fester Stoffe, D-01187 Dresden, Germany
[4] Hochfeld-Magnetlabor Dresden (HLD), Forschungszentrum Dresden-Rossendorf, D-01314 Dresden, Germany

E-mail: M.Schneider@ifw-dresden.de and G.Fuchs@ifw-dresden.de

Received 1 February 2008
Published 7 April 2008
Online at stacks.iop.org/JPhysCM/20/175221

Abstract

For a systematic investigation of the heat- and charge-transport properties of YNi_2B_2C and $HoNi_2B_2C$, single-crystal measurements of the electrical resistivity, the thermal conductivity, and the thermoelectric power were performed on the same samples. For $HoNi_2B_2C$, a local maximum of the Lorenz number at 20 K is evidently connected with the occurrence of magnetic fluctuations well above the ordering temperature. For the in-plane thermal conductivity, a kink near the superconducting transition was observed, consistent with an anisotropic gap or a multiband description. For both investigated borocarbides, the electrical resistance is isotropic. In contrast, the thermal conductivity shows a pronounced anisotropy. The thermoelectric power exhibits a minor anisotropy and can be well described by electron-diffusion and phonon-drag contributions over a wide temperature range. Based on an analysis of full-potential local-orbital calculations, a strong influence of the boron z position on the thermoelectric power has been revealed.

1. Introduction

Rare-earth nickel borocarbides have attracted much interest for more than 10 years because of the rich variety of superconducting and magnetic phenomena depending on the rare-earth ions (for reviews, see [1–3]). A large number of studies have been published with a considerable part devoted to the heat- and charge-transport properties of the borocarbides. Such measurements provide insight into the scattering mechanisms of different excitations. Some recent work on thermoelectric power (TEP) and thermal conductivity properties is reviewed in [4, 5].

Despite the substantial work in this field, a number of questions are still open. In $HoNi_2B_2C$, antiferromagnetic fluctuations well above the magnetic ordering temperature strongly influence the specific heat [6] and the thermal expansion [7] but for the thermal conductivity a fluctuation contribution has never been reported. In the temperature range between the superconducting transition, T_c, and the Néel temperature, T_N, a gapless superconducting state was proposed based on a point-contact study [8] and zero-field thermal conductivity data [9]. Multiband superconductivity, on the other hand, has been shown to be relevant for the non-magnetic borocarbides YNi_2B_2C and $LuNi_2B_2C$, and provides an explanation for a number of properties such as the temperature dependence of the upper critical field [10], results of point-contact spectroscopic measurements [11], and specific heat data in the superconducting state [12]. An indication of a rather large superconducting gap has been suggested from de Haas–van Alphen studies [13]; an anisotropic gap structure has been proposed from photoemission spectroscopy [14].

[5] Present address: Ames Laboratory, Iowa State University, Ames, IA 50011, USA.
[6] Present address: Center for Atomic-scale Materials Design, Department of Physics, Technical University of Denmark, 2800 Kongens Lyngby, Denmark.

To the best of our knowledge, no *c*-axis TEP study for the tetragonal rare-earth nickel borocarbides has been published yet. The available results for polycrystalline samples [15, 16] and for in-plane TEP [4, 17, 18] indicate a strongly anisotropic behaviour, but in some of these studies the sample quality hampers a final conclusion. Furthermore, there is a controversy as to whether a normal phonon-drag contribution exists [15] or whether saturation effects have to be considered [4, 17, 18]. Knowledge of the phonon-drag contribution is of special interest since this would allow us to extract the diffusion part of the TEP. The latter can be compared to band-structure calculations, thus enabling us to estimate the strength of the electron–phonon coupling in the borocarbides.

The availability of large single crystals opened up the possibility of a systematic study of the electrical resistivity, ρ, thermal conductivity, κ, and TEP, S, on the same sample. Here, both in-plane and *c*-axis measurements were performed in order to gain a comprehensive picture of the anisotropic heat and charge transport. For the non-magnetic compound YNi_2B_2C, only contributions from electrons and phonons have to be considered. For $HoNi_2B_2C$, the influence of magnetic excitations also has to be taken into account. In this paper, after presenting electrical resistance data, results of thermal conductivity data and of TEP measurements are discussed.

2. Technical details

The investigated $RNi_2{}^{11}B_2C$ single crystals, where R = Y or Ho, were grown by a vertical floating-zone-melting technique as described elsewhere [19]. Different pieces of approximately 6 mm in length, oriented parallel to one of the main crystallographic directions, and of a cross-section of 2×2 mm^2 were cut from the same crystal. In the case of $HoNi_2B_2C$, the samples were used for a thermal-expansion study as well [7]. The sample orientation was determined using x-ray Laue back scattering.

The electrical resistance and the thermal conductivity were measured by the usual four-point method and by the standard steady-state method, respectively. The thermal conductivity was measured simultaneously with the TEP using copper wires as voltage contacts and AuFe–Chromel thermocouples for measuring the temperature differences. The temperature gradient along the sample of about 1% of the average temperature was generated by a small strain-gauge heater.

We applied the full-potential local-orbital (FPLO) code (version 5.00-18) [20] in its scalar relativistic version within the local density approximation (LDA) to calculate the density of states (DOS) of YNi_2B_2C. For exchange and correlation potentials the Perdew–Wang form [21] was used. The basis set was chosen to be Y(4s, 4p, 4d, 5s, 5p), Ni(3s, 3p, 3d, 4s, 4p), B(2s, 2p, 3d), and C(2s, 2p, 3d). Lattice parameters $a = b$ and c were taken from [22], the B position was varied within the range of the experimental data provided by [22–26]. To ensure significance of the theoretical results, careful convergence tests with regard to the k sampling were performed, resulting in us finally using 6348 k points in the irreducible part of the Brillouin zone.

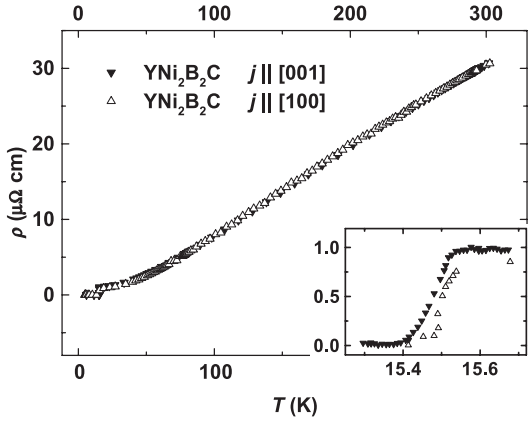

Figure 1. Temperature dependence of the electrical resistivity ρ of YNi_2B_2C for currents parallel and perpendicular to the *c*-axis. The inset shows the data near T_c on an enlarged scale.

3. Results and discussion

3.1. Electrical resistivity

The electrical resistivity, ρ, of YNi_2B_2C (figure 1) shows a metallic behaviour with a linear increase for temperatures above 150 K. The resistivity ratio between ρ at 300 K and just above $T_c = 15.5$ K is about 40, a rather high value among those reported so far. The good quality and homogeneity of the sample is further underlined by the sharp resistive transition to the superconducting state occurring within 100 mK (inset of figure 1). The measured ρ for both crystallographic directions agrees within experimental uncertainty, which is mainly governed by the geometry factor (about 10%). For a better comparison, all resistivity data shown here are scaled by a few per cent in such a way that the room-temperature values correspond to each other.

The resistivity data between T_c and about 70 K can be well described by the expression

$$\rho(T) = \rho_0 + AT^n. \tag{1}$$

There is a small but distinctive difference between the residual resistivities for the two current directions as can be seen in the inset of figure 2; $\rho_0 = 0.85$ $\mu\Omega$ cm for current along c and $\rho_0 = 0.70$ $\mu\Omega$ cm for current along the a direction. After subtraction of ρ_0, the power-law dependence can be seen in figure 2. The fit (1) yields $A = 3 \times 10^{-4}$ $\mu\Omega$ cm K^{-n} and $n = 2.2$ for both current directions. Such a temperature dependence has previously been reported in [17, 27]. In the latter study, a strongly sample-dependent value of A was found. This feature has also been observed for other superconductors, such as organic compounds [28] and MgB_2 [29]. In the latter case this might be explained by multiband effects [30].

In a previous report the resistivity data could be described by the usual Bloch–Grüneisen law [31] and in another report a modified expression has been used [32]. Our data are, however, best described by the above power law with $n = 2.2$. The origin of this characteristic temperature dependence has not been understood yet. Several possible mechanisms, including electron–electron interaction, strong electron–phonon coupling

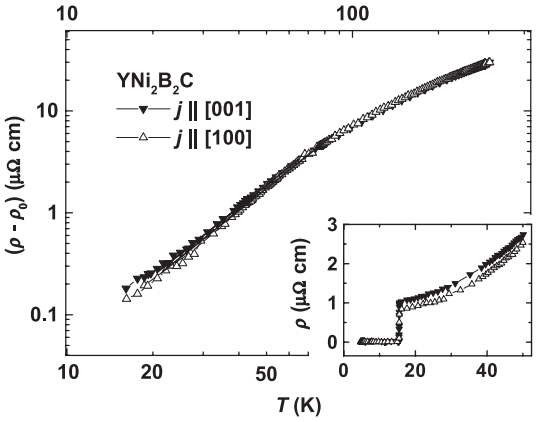

Figure 2. Log–log plot of the data shown in figure 1 after subtraction of the residual resistivities. The inset shows $\rho(T)$ below 50 K.

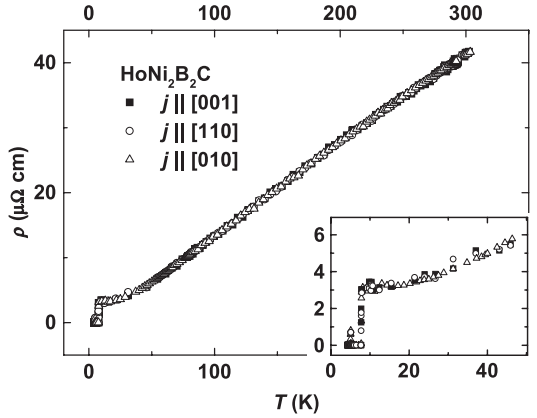

Figure 3. Temperature dependence of the electrical resistivity of $HoNi_2B_2C$ for current flows parallel to different crystal axes. The values are scaled by a few per cent as described in the text. The inset shows the data below 50 K on an enlarged scale.

in disordered samples, electron–electron correlation effects, or valence fluctuations have been suggested [17, 33].

The resistivity of $HoNi_2B_2C$ shows no anisotropies for the measurements with currents parallel to the three main crystallographic directions (figure 3). This is in contrast to previous results [34, 35] reflecting a small but significant anisotropy in the low-temperature resistivity of $HoNi_2B_2C$. Our result supports the suggestion of a fundamentally isotropic resistivity [35] and suggests possible crystal imperfections as the origin for the observed anisotropies. The physical properties of the borocarbides depend sensitively on small deviations from exact stoichiometry, especially in the case of $HoNi_2B_2C$ [36].

The sharp superconducting transition at 7.8 K with a very narrow width of less than 100 mK underlines the good homogeneity of our sample. The moderate T_c and the appearance of a zero-field reentrant signal near $T_N = 5.2$ K are common in as-grown crystals. The low-temperature resistivity and especially the reentrant signal strongly depend on the annealing procedure [37–39]. The resistivity ratio $\rho(300\ \text{K})/\rho(10\ \text{K}) = 15$ is significantly smaller than that of YNi_2B_2C. This is most probably caused by additional

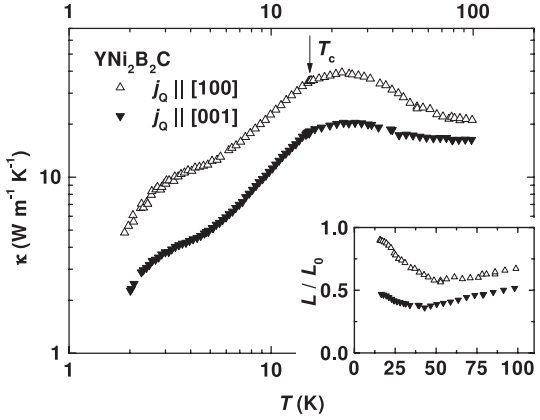

Figure 4. Log–log plot of the thermal conductivity κ of YNi_2B_2C for heat flows parallel and perpendicular to the c-axis. The inset shows the reduced Lorenz number calculated from resistivity and heat-transport data.

scattering at magnetic fluctuations at low temperatures in $HoNi_2B_2C$.

In the range 20 K $< T <$ 55 K the data can be well described by (1) with $\rho_0 = 2.8\ \mu\Omega$ cm, $A = 6 \times 10^{-4}\ \mu\Omega$ cm K^{-n}, and $n = 2.2$. The exponent is in good agreement with previous reports for n ranging between 2.0 and 2.6 [18, 40–42]. The residual resistivity ρ_0 is one of the lowest zero-field values for $HoNi_2B_2C$ reported so far. Thus, the remaining disorder in as-grown samples strongly affects the superconducting properties but has a minor influence on the normal-state transport.

3.2. Thermal conductivity

The thermal conductivity, κ, of YNi_2B_2C, shown in figure 4, agrees well with previous reports [5, 43–45]. Its in-plane values are approximately twice as large as the c-axis κ in the whole measured temperature range, in agreement with the data reported in [43], despite a larger anisotropy at the lowest measured temperatures. Considering the fundamentally isotropic resistivity, this result points to a remarkably anisotropic phonon spectrum. At T_c, a clear slope change is apparent in κ. The enhanced reduction of κ below T_c reflects the role of the electrons as heat carriers and scattering centres in YNi_2B_2C. Towards lower temperatures a moderately enhanced phonon-induced contribution appears near 3 K. The absence of a general correlation between this enhancement and the sample quality was reported for niobium samples [46]. A more detailed discussion of the thermal conductivity of non-magnetic borocarbides, including the behaviour at very low temperatures, is given in [5].

In the inset of figure 4, the Lorenz number,

$$L(T) = \frac{\kappa(T)\rho(T)}{T}, \tag{2}$$

divided by the Sommerfeld value $L_0 = 2.44 \times 10^{-8}$ W Ω K^{-2} is shown. The resulting $L/L_0 < 1$ points to different scattering mechanisms in ρ and κ with dominating electronic heat conduction. The minima in L/L_0 are more pronounced

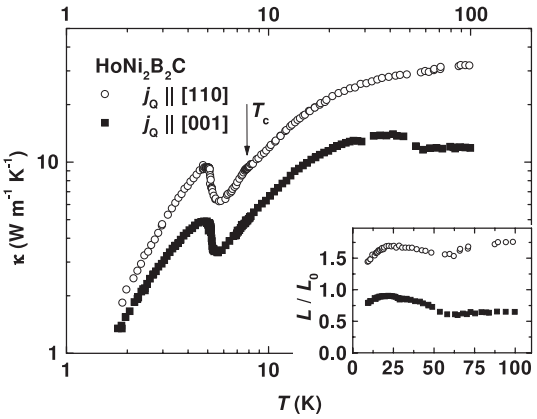

Figure 5. Log–log plot of the thermal conductivity of $HoNi_2B_2C$ for heat flows parallel and perpendicular to the c-axis. The inset shows the reduced Lorenz number.

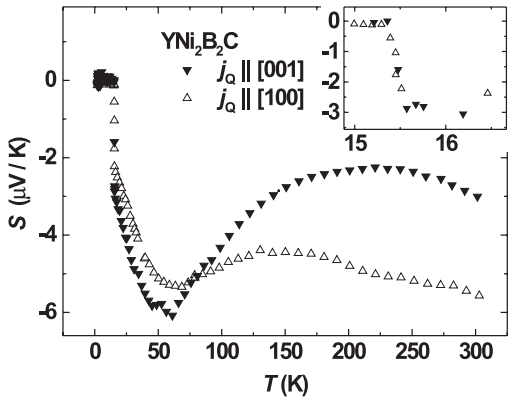

Figure 6. Thermoelectric power S of YNi_2B_2C for heat flows parallel and perpendicular to the c-axis. The inset shows the data close to T_c on an enlarged scale.

than those reported in [43] and quite similar to that observed for $LuNi_2B_2C$ [47]. In the latter study, a correlation between the depth of the minima and a low residual resistivity was pointed out, in line with our observations.

The thermal conductivity of $HoNi_2B_2C$ (figure 5) agrees in the main features with κ previously reported [5, 9, 43, 48]. There are, however, some characteristic differences for the in-plane heat transport. At T_c, our measured κ is larger than previously observed. In our data we are able to resolve a kink of $\kappa(T)$ close to T_c. The previously proposed [9] gapless superconductivity based on a magnetic-fluctuation mechanism [49] in the range between T_N and T_c was assumed not to show such a kink. Its experimental resolution is most probably related to the high quality of our crystal. Interestingly, a similar kink near T_c seems also to be present in the data measured by Belevtsev *et al* [5]. Possible explanations for the missing kink structure in the c-axis measurement presented here are the reduced κ as well as the existence of an anisotropic gap, as mentioned above.

At T_N, well below T_c, the strongly enhanced thermal conductivity points to an unusually high fraction of free electrons, consistent with a decoupled multiband model with different T_c-values [39, 50]. As evidenced by neutron-scattering data, an incommensurate magnetic structure evolves slightly above T_N at about 6 K [51]. In our thermal conductivity data no definitive feature related to this phase transition can be resolved.

The inset of figure 5 shows the temperature dependence of L for $HoNi_2B_2C$. Considering the isotropic behaviour of ρ, the differences in $L(T)$ for both crystallographic directions originate from different phonon contributions to κ. The phonon heat conduction is especially large for the in-plane heat transport as indicated by $L/L_0 > 1$. The stronger in-plane phonon contribution to κ in $HoNi_2B_2C$ compared with that in YNi_2B_2C is in line with the results of [5]. A possible influence of crystalline-electric-field effects on the phonon system in $HoNi_2B_2C$ should be further investigated in magnetic fields.

$L(T)$ reveals a local minimum at 60 K, as also observed for YNi_2B_2C (see inset of figure 4), and in addition a maximum at about 20 K, not observed for the non-magnetic borocarbides. The reduction of L/L_0 below about 20 K cannot be explained by resistive effects. A reasonable assumption is that antiferromagnetic fluctuations in $HoNi_2B_2C$ lead to an enhanced electron scattering (in comparison with YNi_2B_2C), which is more effective in κ than in ρ. Such fluctuations well above T_N lead to local minima in the specific heat and in the thermal expansion at about 14 K [6, 7].

3.3. Thermoelectric power

The TEP, S, of YNi_2B_2C (figure 6) is negative in the normal state, indicating an electronic character of the charge carriers [52]. This is in line with Hall-effect studies [1]. At T_c, S sharply drops to zero (inset of figure 6).

The difference between the in-plane and the c-axis TEP is much smaller than expected from previous results obtained for polycrystalline samples [15, 16] and in-plane measurements [4, 17]. Whereas in our study the in-plane TEP at room temperature is smaller than reported in [17], our powder-averaged value of nearly $-5\ \mu V\ K^{-1}$ is larger than the result obtained in [15] and comparable to that reported in [16]. These diverging data point to a strong sample dependence of S. Indeed, for $YbNi_2B_2C$, S was reduced by about 25% at room temperature by an annealing procedure [53]. The minimum in S at about 60–70 K (figure 6) depends on crystal properties but has also been observed, although less pronounced, for a polycrystalline sample [15].

In order to clarify whether the high-temperature TEP might be explained by a phonon-drag contribution we analysed our data using the expression

$$S(T) = S_g + S_d = \frac{A}{T} + BT, \tag{3}$$

where A and B are fitting parameters for the phonon-drag (S_g) and the electron-diffusion (S_d) term, respectively. An excellent description of the in-plane data is possible using (3) in the range $90\,K < T < 300\,K$ with $A = -340\ \mu V$ and $B = -15\ nV\ K^{-2}$ (figure 7). For S measured along the c-axis only the data above 240 K follow the above expression.

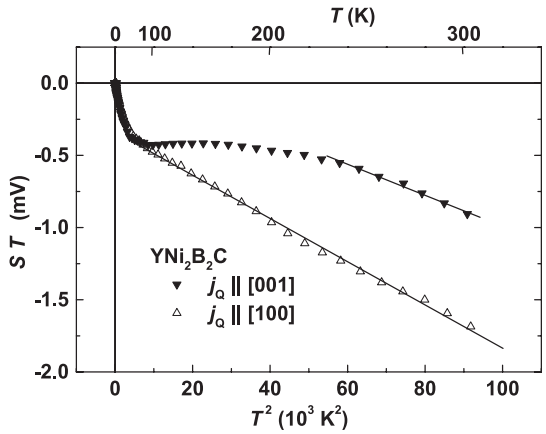

Figure 7. Thermoelectric power of YNi_2B_2C plotted as ST versus T^2. The lines represent fits to the data according to (3) in the ranges 90 K $< T <$ 300 K and 240 K $< T <$ 300 K, respectively.

Here, $A = 80\ \mu$V and $B = -11$ nV K^{-2} are obtained. These fitting parameters are in general agreement with the mentioned study of a polycrystalline sample [15]. The in-plane S data above 170 K reported in [17] can be well reproduced by (3) with $A = -550\ \mu$V and $B = -22$ nV K^{-2}. Notably, no indication for a saturation of the phonon-drag TEP [17] was found in the present study.

The electron-diffusion TEP in the single-band picture is described by the Mott formula renormalized by the electron–phonon coupling constant λ_{ep} [54],

$$S_d(T) = \frac{\pi^2 k_B^2 T}{3e}\left[\frac{\partial \ln \sigma(\varepsilon)}{\partial \varepsilon}\right]_{E_F}(1+\lambda_{ep}(T)), \qquad (4)$$

where the logarithmic energy derivative of the electrical conductivity σ has to be evaluated at the Fermi level E_F. S_d extracted from band-structure calculations [55] using the single-band description for the total electronic density of states (as well as a single scattering rate) seems to yield unrealistically large TEP values compared to the experimental data [15]. A possible reason for this discrepancy is the multiband nature of the superconductivity. Thus, the contributions from different bands to the electrical conductivity have to be evaluated separately before adding up. The scattering rates are assumed to be independent of the energy and interband scattering has been ignored for the sake of simplicity. (Note that for the non-superconducting $LaNi_2B_2C$ a possible Fermi-energy shift away from the maximum in the electronic density of states has been discussed [15].)

The strongly sample-dependent TEP discussed above gave reasons for further analysis taking into account possible small microscopic differences between those crystals. Varying the lattice parameters in the range of reported experimental values [22–26] ($a = b = 3.5295$ Å $\pm$ 0.0035 Å, $c =$ 10.551 Å $\pm$ 0.015 Å) does not remarkably affect the calculated total electronic density of states, DOS, whereas the variation of the boron position z_B in the range of values of the same reports ($z_B = 0.3531 \ldots 0.3592$) reveals a strong sensitivity of the

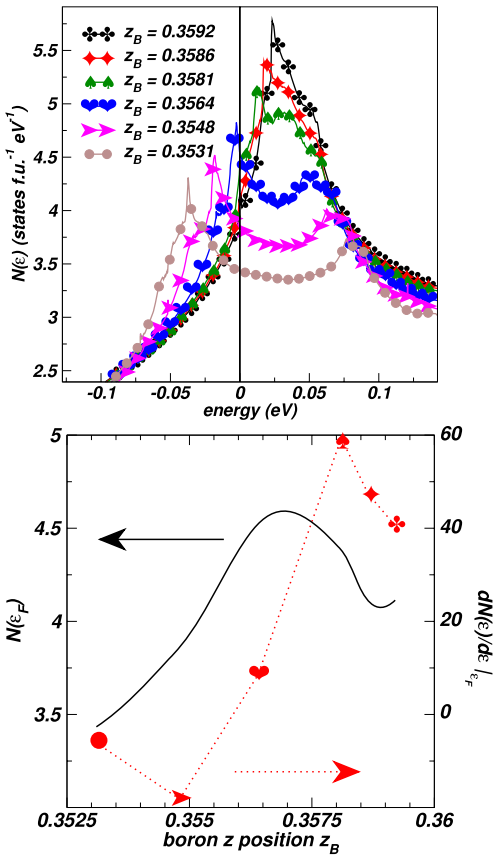

Figure 8. Upper panel: calculated total DOS of YNi_2B_2C for different Wyckoff boron z positions z_B (lattice parameters a, b, c from [22]). Symbols are shown for a few of the calculated values (lines) only. The straight line (at zero energy) marks the Fermi level. Lower panel: total DOS (smooth black, solid line) and its energy derivative (red, dotted line; symbols according to those in the upper plot) at the Fermi level, depending on z_B.

(This figure is in colour only in the electronic version)

total and the partial DOS on this parameter[7]. The upper panel of figure 8 displays the total DOS $N(\varepsilon)$ in close vicinity of the Fermi level for z_B in the mentioned range of experimental values. The lower panel illustrates the influence of the boron z position on the total DOS and its energy derivative at the Fermi level. The resulting strong dependence of the TEP on small variations of this crystallographic parameter and the multiband nature of the Fermi surface do not only explain the apparent contradiction between the experimental results and the previous theoretical calculations but also the remarkable scattering of S values for different samples, as discussed above. It should be noted that, for some of the z_B values, different bands exhibit even a different sign of the contributions to the energy derivative. Thus, the TEP can provide sensitive information which might give constraints for the boron position in stoichiometric YNi_2B_2C. A further

[7] It should be emphasized that the calculations are based on the experimental data. The sample dependence of the properties of $HoNi_2B_2C$ connected with boron–carbon disorder [36] suggests that such a z_B variation in the borocarbides might result from details of the crystal growth. A detailed description would have to treat such disorder effects in the frame of the coherent-potential approximation.

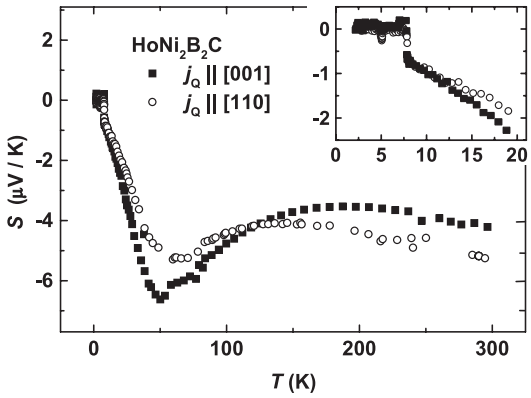

Figure 9. Thermoelectric power of $HoNi_2B_2C$ for heat flows parallel and perpendicular to the c-axis. The inset shows the temperature range below 20 K on an enlarged scale.

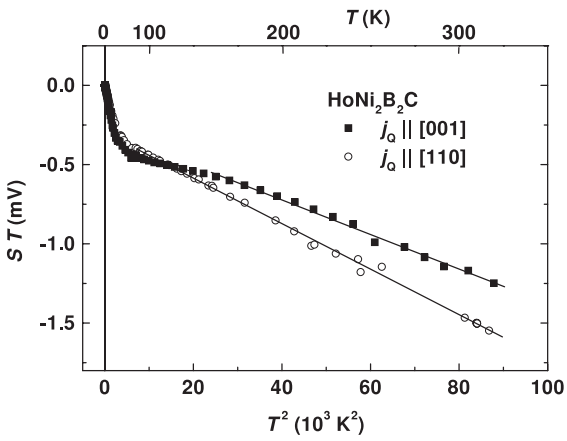

Figure 10. The data shown in figure 9 plotted as ST versus T^2. The lines represent fits to the data according to (3) for 70 K $< T <$ 300 K and 150 K $< T <$ 300 K, respectively.

possibility for studying the influence of the lattice constants on S is the investigation of the pressure-dependent TEP, as demonstrated at room temperature in [56].

The TEP of $HoNi_2B_2C$ (figure 9) resembles very much the data for the non-magnetic YNi_2B_2C discussed above. The only principal difference is the reentrant behaviour in a narrow range near T_N (inset of figure 9), in line with the resistivity data shown in figure 3 above.

The in-plane TEP at 300 K is somewhat smaller than the value reported in [18], but the powder-averaged value agrees well with a study on a polycrystalline sample [15]. The anisotropy in S is weaker than in the case of YNi_2B_2C. The TEP data of $HoNi_2B_2C$ can be well described by (3) in a wide range up to 300 K (figure 10).

The fit yields $A = -300\ \mu$V for both measured directions and $B = -14$ nV K^{-2} ($B = -11$ nV K^{-2}) for the in-plane (c-axis) heat transport. No saturation effects in the phonon-drag contribution are observed in contrast to a previous study [18]. Comparing the results for $HoNi_2B_2C$ and YNi_2B_2C, the electron-diffusion terms are found to agree in both magnitude and anisotropy, whereas the phonon drag characterized by A differs for the c-axis TEP. The latter might point to differences in the phonon system between the two compounds.

4. Summary

For both investigated borocarbides, YNi_2B_2C and $HoNi_2B_2C$, the normal-state resistivities are isotropic within error bars and can be described by a power-law dependence over a wide temperature range. In $HoNi_2B_2C$, antiferromagnetic fluctuations well above the ordering temperature are visible in the data of the electrical resistivity, ρ, and the thermal conductivity, κ, leading to a local maximum in the Lorenz number. A kink in κ near T_c points to a multiband character of the superconducting state or a highly anisotropic gap, but is at odds with previous results interpreted in terms of a gapless superconducting state above T_N. For both borocarbides, κ exhibits a significant anisotropy between the basal plane and the c-axis by a factor of about 2. The TEP, S, on the other hand, shows only a moderate anisotropy. The temperature dependence of S can be well described by an electron-diffusion and a phonon-drag term at high temperatures. No saturation was observed for the latter contribution. The electron-diffusion contribution of both investigated materials is identical within error bars. The calculated magnitude of this contribution is found to depend sensitively on the boron z position. This underlines the importance of further studies on well-characterized crystals.

Acknowledgments

This work has been supported by the DFG through the Sonderforschungsbereich 463. We acknowledge valuable discussions with D Lipp, Yu G Naidyuk, and O E Kvitnitskaya.

References

[1] Müller K-H and Narozhnyi V N 2002 *Rep. Prog. Phys.* **64** 943
[2] Bud'ko S L and Canfield P C 2006 *C. R. Physique* **7** 56
[3] Müller K-H, Schneider M, Fuchs G and Drechsler S-L 2007 *Handbook on the Physics and Chemistry of Rare Earths* vol 38, ed K A Gschneidner Jr, J-C G Bünzli and V K Pecharsky (Amsterdam: Elsevier) chapter 239 p 175
[4] Naugle D G, Rathnayaka K D D and Bhatnagar A K 1999 *Studies of High Temperature Superconductors* vol 28, ed A V Narlikar (Commack: Nova Science) p 189
[5] Belevtsev B I, Hennings B D, Rathnayaka K D D and Naugle D G 2003 *Studies of High Temperature Superconductors* vol 46, ed A V Narlikar (Commack: Nova Science) p 99
[6] Carter S, Batlogg B, Cava R, Krajewski J and Peck W F Jr 1995 *Phys. Rev.* B **51** 12644
[7] Schneider M, Gladun A, Kreyssig A, Wosnitza J, Souptel D and Behr G 2007 *J. Magn. Magn. Mater.* **311** 489
[8] Rybaltchenko L F, Janson A G M, Wyder P, Tjutrina L V, Canfield P C, Tomy C V and Paul D McK 1999 *Physica* C **319** 189
[9] Hennings B D, Naugle D G and Canfield P C 2002 *Phys. Rev.* B **66** 214512
[10] Shulga S V, Drechsler S-L, Fuchs G, Müller K-H, Winzer K, Heinecke M and Krug K 1998 *Phys. Rev. Lett.* **80** 1730
[11] Bashlakov D L, Naidyuk Yu G, Yanson I K, Wimbush S C, Holzapfel B, Fuchs G and Drechsler S-L 2005 *Supercond. Sci. Technol.* **18** 1094

[12] Huang C L, Lin J-Y, Sun C P, Lee T K, Kim J D, Choi E M, Lee S I and Yang H D 2006 *Phys. Rev.* B **73** 012502
[13] Ignatchik O, Coffey T, Hagel J, Jobiliong E, Souptel D, Behr G and Wosnitza J 2005 *J. Magn. Magn. Mater.* **290/291** 424
[14] Baba T *et al* 2006 *Physica* B **378–380** 469
[15] Fisher I R, Cooper J R and Cava R J 1995 *Phys. Rev.* B **52** 15086
[16] Lee J H, Ha Y S, Song Y S, Park Y W and Choi Y S 1996 *Proc. 10th Anniversary HTS Workshop in Physics, Materials and Applications* ed B Batlogg *et al* (Singapore: World Scientific) p 332
[17] Rathnayaka K D D, Bhatnagar A K, Parasiris A, Naugle D G, Canfield P C and Cho B K 1997 *Phys. Rev.* B **55** 8506
[18] Bhatnagar A K, Rathnayaka K D D, Naugle D G and Canfield P C 1997 *Phys. Rev.* B **56** 437
[19] Souptel D, Behr G, Kreyssig A and Löser W 2005 *J. Cryst. Growth* **276** 652
Behr G and Löser W 2005 *Recent Res. Dev. Cryst. Growth* **4** 129
[20] Koepernik K and Eschrig H 1999 *Phys. Rev.* B **59** 1743
[21] Perdew J P and Wang Y 1992 *Phys. Rev.* B **45** 13244
[22] Wong-Ng W, Cava R J, Krajewski J J and Peck W F Jr 1996 *Powder Diffr.* **11** 88
[23] Jaenicke-Roessler U, Belger A, Zahn G, Wehner B, Paufler P and Bitterlich H 1999 *Physica* C **314** 43
[24] Godart C *et al* 1995 *Phys. Rev.* B **51** 489
[25] Siegrist T, Cava R J, Krajewski J J and Peck W F Jr 1994 *J. Alloys Compounds* **216** 135
[26] Hong N M, Michor H, Vybornov M, Holubar T, Hundegger P, Perthold W, Hilscher G and Rogl P 1994 *Physica* C **227** 85
[27] Lipp D, Gladun A, Bartkowski K, Belger A, Paufler P and Behr G 2000 *Physica* B **284–288** 1103
[28] Strack Ch *et al* 2005 *Phys. Rev.* B **72** 054511
[29] Schneider M, Lipp D, Gladun A, Zahn P, Handstein A, Fuchs G, Drechsler S-L, Richter M, Müller K-H and Rosner H 2001 *Physica* C **363** 6 and references therein
[30] Mazin I I and Antropov V P 2003 *Physica* C **385** 49
[31] Gonnelli R S, Morello A, Ummarino G A, Stepanov V A, Behr G, Graw G, Shulga S V and Drechsler S-L 2000 *Int. J. Mod. Phys.* B **14** 2840
Gonnelli R S, Morello A, Ummarino G A, Stepanov V A, Behr G, Graw G, Shulga S V and Drechsler S-L 2000 *Physica* C **341–348** 1957
[32] Andreone A, Fontana F, Iavarone M, Vaglio R, Canepa F, Manfrinetti P and Palenzona A 1995 *Physica* C **251** 379
[33] Brandow B 2000 *Phil. Mag.* B **80** 1229
[34] Fisher I R, Cooper J R, Locherer K R, Cava R J and Canfield P C 1996 *J. Low Temp. Phys.* **105** 1623
[35] Fisher I R, Cooper J R and Canfield P C 1997 *Phys. Rev.* B **56** 10820
[36] Schmidt H, Weber M and Braun H F 1996 *Physica* C **256** 393
Schmidt H and Braun H F 1998 *Studies of High Temperature Superconductors* vol 26, ed A V Narlikar (Commack: Nova Science) p 47
Dertinger A, Dinnebier R E, Kreyssig A, Stephens P W, Pagola S, Loewenhaupt M, van Smaalen S and Braun H F 2000 *Phys. Rev.* B **63** 184518
[37] Durán A, Muñoz E, Bernès S and Escudero R 2000 *J. Phys.: Condens. Matter* **12** 7595
[38] Miao X Y, Bud'ko S L and Canfield P C 2002 *J. Alloys Compounds* **338** 13
[39] Müller K-H *et al* 2007 *Physica* C **460–462** 99
[40] Oomi G, Matsuda N, Kagayama T, Cho C K and Canfield P C 2003 *Int. J. Mod. Phys.* B **17** 3664
[41] Ohashi M, Akiyama H, Oomi G, Cho B K and Canfield P C 2004 *J. Magn. Magn. Mater.* **272–276** 263
[42] Akiyama H, Kaji S, Oomi G, Cho B K and Canfield P C 2006 *J. Alloys Compounds* **408–412** 226
[43] Sera M, Kobayash S, Hiroi M, Kobayashi N, Takeya H and Kadowaki K 1996 *Phys. Rev.* B **54** 3062
[44] Hennings B D, Rathnayaka K D D, Naugle D G and Canfield P C 2000 *Physica* C **341–348** 753
[45] Izawa K, Kamata K, Nakajima Y, Matsuda Y, Watanabe T, Nohara M, Takagi H, Thalmeier P and Maki K 2002 *Phys. Rev. Lett.* **89** 137006
[46] Gladun A, Gladun C, Knorn M and Vinzelberg H 1977 *J. Low Temp. Phys.* **27** 873
[47] Boaknin E, Hill R W, Lupien C, Taillefer L and Canfield P C 2000 *Physica* C **341–348** 1845
[48] Cao S, Sakai S, Nishimura K and Mori K 2001 *IEEE Trans. Appl. Supercond.* **11** 3603
[49] Ambegaokar V and Griffin A 1965 *Phys. Rev.* **137** A1151
[50] Naidyuk Yu G, Kvitnitskaya O E, Yanson I K, Fuchs G, Nenkov K, Wälte A, Behr G, Souptel D and Drechsler S-L 2007 *Phys. Rev.* B **76** 014520
[51] Lynn J W, Skanthakumar S, Huang Q, Sinha S K, Hossain Z, Gupta L C, Nagarajan R and Godart C 1997 *Phys. Rev.* B **55** 6584
[52] Barnard R D 1972 *Thermoelectricity in Metals and Alloys* (London: Taylor and Francis)
Blatt F J, Schroeder P A, Foiles C L and Greig D 1976 *Thermoelectric Power of Metals* (New York: Plenum)
[53] Avila M A, Bud'ko S L and Canfield P C 2002 *Phys. Rev.* B **66** 132504
[54] Kaiser A B and Uher C 1991 *Studies of High Temperature Superconductors* vol 7, ed A V Narlikar (Commack: Nova Science) p 353
[55] Mattheiss L F 1994 *Phys. Rev.* B **49** 13279
Lee J I, Zhao T S, Kim I G, Min B I and Youn S J 1994 *Phys. Rev.* B **50** 4030
Pickett W E and Singh D J 1994 *Phys. Rev. Lett.* **72** 3702
Mattheiss L F, Siegrist T and Cava R J 1994 *Solid State Commun.* **91** 587
Coehoorn R 1994 *Physica* C **228** 331
Kim H, Hwang C and Ihm J 1995 *Phys. Rev.* B **52** 4592
Ravindran P, Johannson B and Erikson O 1998 *Phys. Rev.* B **58** 3381
[56] Meenakshi S, Vijayakumar V, Rao R S, Godwal B K, Sikka S K, Ravindran P, Hossain Z, Nagarajan R, Gupta L C and Vijayaraghavan R 1998 *Phys. Rev.* B **58** 3377